Predicting Correlation Coefficients for Monte Carlo Eigenvalue Simulations

Jilang Miao* Benoit Forget* Kord Smith*

*Massachusetts Institute of Technology, 77 Massachusetts Ave, Cambridge, MA 02139
jlmiao@mit.edu, bforget@mit.edu, kord@mit.edu

INTRODUCTION

Monte Carlo methods are most often considered as a reference for neutron transport simulations since very limited approximations are made abount nuclear data and system geometry. To report uncertainty of any tally evaluated as generation averages, the sample variance is divided by the number of active generations, which is based on the assumption that the neutron generations are independent. Correlation effects between neutrons in multiplying systems, particularly when performing power iteration to evaluate eigenvalues have been observed in previous work [1] [2] [3] [4]. Neglecting the correlation effect results in an underestimate of uncertainty reported by Monte Carlo calculations. Previous work has also proposed methods to predict the underestimation ratio. Yamamoto et al [5] expanded the fission source distribution with diffusion equation modes, performed numerical simulation of the AR(autoregressive) process of the expansion coefficients and used the correlation of the AR process to predict that of the Monte Carlo eigenvalue simulation. Sutton [6] applied the discretized phase space (DPS) approach to predict the underestimation ratio but the method cannot predict the ratio when one neutron generates offspring in different phase space regions or generates a random number of offspring.

This paper presents a method to predict the correlation effect with the model of multitype branching processes (MBP) [7]. The method requires simulations for one generation of neutrons without knowing the source distribution and can predict the underestimation ratio for the cases where the traditional DPS approach does not work.

The generation-to-generation correlation determines the convergence rate of active generations, the bias of variance estimator for each generation and the underestimation ratio of variance estimator for tallies averaged over active generations [4]. The generation-to-generation correlation is characterized by the Auto-Correlation Coefficients (*ACC*) between tallies from different generations.

THEORY

Suppose generation n yields tally $X_l(n)$ for tally region l, the simulation will report the average $\bar{X}_l = \sum_{i=1}^{N} X_l(i)/N$ and σ_{X_l}/N as an approximation of $\sigma_{\bar{X}_l}$. Due to the correlation, σ_{X_l}/N underestimates $\sigma_{\bar{X}_l}$. The $Cov[X_l(i), X_l(j)]$, where i,j are the active generation indexes, is required to correct the underestimated uncertainty.

The generation-to-generation correlation results from the fission source update procedure where the source of generation $n+1$ is sampled from the fission sites of generation n. And the correlation of other tallies can be calculated from the correlation of fission source distribution [8].

Theory of Multitype Branching Processes

The model of multitype branching process discretizes the neutron phase space in space, angle and energy into m discrete regions and denotes the system state at generation n with a vector $\boldsymbol{Z}(n)$. The l^{th} component of the vector corresponds to the number of neutrons belonging to region l at generation n. A neutron in discretized phase space region l is defined to be of type l.

$$\boldsymbol{Z}(n) = (Z_1(n), \cdots, Z_l(n), \cdots, Z_m(n)) \tag{1}$$

The state vector at generation n are related with that of generation $n-1$ through

$$\boldsymbol{Z}(n) = \sum_{i=1}^{m} \sum_{j=1}^{Z_i(n-1)} \boldsymbol{Y}_{ij} \tag{2}$$

where $\boldsymbol{Y_{ij}}$ is the state vector generated by the j^{th} neutron of type i at generation $n-1$.

The moment generating function of $\boldsymbol{Z}(n)$ is defined as

$$F_n(\boldsymbol{r}_0, \boldsymbol{s}) = \sum_{\boldsymbol{r}} \mathbb{P}\left(\boldsymbol{Z}(n) = \boldsymbol{r} | \boldsymbol{Z}(0) = \boldsymbol{r}_0\right) \prod_{i=1}^{m} s_i^{r_i} \tag{3}$$

where $\boldsymbol{r}_0$ denotes the initial configuration of neutrons in the discretized phase space. Thus, if $\boldsymbol{r}_0$ is point source of type i, we can denote $F_n(\boldsymbol{r}_0, \boldsymbol{s})$ as $F_n(i, \boldsymbol{s})$. It can also be shown that

$$F_n(\boldsymbol{r}_0, \boldsymbol{s}) = \prod_{i=1}^{m} F_n(i, \boldsymbol{s})^{r_0^i} \tag{4}$$

$F_n(i, \boldsymbol{s})$ can be evaluated from $F_1(i, \boldsymbol{s})$ recursively by defining the vector of function $\boldsymbol{f}(n, \boldsymbol{s})$ as in Eq 5:

$$\begin{aligned} \boldsymbol{f}(1, \boldsymbol{s}) &= (F_1(1, \boldsymbol{s}), \cdots, F_1(m, \boldsymbol{s})) \\ \boldsymbol{f}(n, \boldsymbol{s}) &= \boldsymbol{f}(n-1, \boldsymbol{f}(1, \boldsymbol{s})) \end{aligned} \tag{5}$$

$$F_n(i, \boldsymbol{s}) = (\boldsymbol{f}(n, \boldsymbol{s}))_i \tag{6}$$

where $F_n(i, \boldsymbol{s})$ is the i^{th} component of the vector $\boldsymbol{f}(n, \boldsymbol{s})$.

The spatial moments of $Z_l(n)$ such as $\mathbb{E}[Z_l(n)]$, $\mathbb{E}[Z_l(n)Z_j(n)]$ and $\mathbb{E}[Z_l(n)Z_j(n)Z_k(n)]$, denoted by $\mu_l(n)$, $C_{l,j}(n)$ and $T_{l,j,k}(n)$ respectively, can be evaluated by taking derivatives of $F_n(\boldsymbol{r}_0, \boldsymbol{s})$. The recursive relation (Eq 5) yields the evolution of the spatial moments:

$$\begin{aligned} \mu_i(n+1) &= \mu_l(n) M_i^l \\ C_{i,j}(n+1) &= M_i^l C_{l,h}(n) M_j^h + V_{i,j}^l \mu_l(n) \\ T_{k,j,i}(n+1) &= T_{g,h,l}(n) M_k^g M_j^h M_i^l + V_{j,i}^l M_k^\alpha C_{l,\alpha}(n) \\ &\quad + V_{k,i}^l M_j^\alpha C_{l,\alpha}(n) + V_{j,k}^l M_i^\alpha C_{l,\alpha}(n) + W_{i,j,k}^l \mu_l(n) \end{aligned} \tag{7}$$

where the Einstein tensor notation is used (the sum is taken over all values of the index whenever the same symbol appears as a subscript and superscript in the same term). M_i^l, $V_{i,j}^l$ and $W_{i,j,k}^l$ are defined as the first, second and third spatial moment responses to a point source integrated over phase space cell l:

$$\begin{aligned} M_i^l &= \mathbb{E}[Z_i(1)|(\boldsymbol{r}_0)_h = \delta_{l,h}] \\ V_{i,j}^l &= \mathbb{E}[(Z_i(1)-\mu_i(1))(Z_j(1)-\mu_j(1))|(\boldsymbol{r}_0)_h = \delta_{l,h}] \\ W_{i,j,k}^l &= \\ \mathbb{E}[(Z_i(1)-\mu_i(1))&(Z_j(1)-\mu_j(1))(Z_k(1)-\mu_k(1))|(\boldsymbol{r}_0)_h = \delta_{l,h}] \end{aligned} \tag{8}$$

To calculate the generation-to-generation correlation, the joint moment generating function of $\boldsymbol{Z}(n)$ and $\boldsymbol{Z}(n+k)$ is also required (where k is the fission source lag):

$$\begin{aligned} &F_{n,n+k}(\boldsymbol{r}_0, \boldsymbol{s}, \boldsymbol{t}) = \\ &\sum_{\boldsymbol{r},\boldsymbol{q}} \mathbb{P}(\boldsymbol{Z}(n) = \boldsymbol{r}, \boldsymbol{Z}(n+k) = \boldsymbol{q}|\boldsymbol{Z}(0) = \boldsymbol{r}_0) \prod_{i=1}^{m} s_i^{r_i} t_i^{q_i} \end{aligned} \tag{9}$$

The joint moment generating function $F_{n,n+k}(\boldsymbol{r}_0, \boldsymbol{s}, \boldsymbol{t})$ satisfies the functional equation

$$\begin{aligned} F_{n,n+k}(\boldsymbol{r}_0, \boldsymbol{s}, \boldsymbol{t}) &= F_n(\boldsymbol{r}_0, \boldsymbol{u}(k)) \\ u_i(k) &= s_i F_k(i, \boldsymbol{t}) \end{aligned} \tag{10}$$

Approximating the *ACC*s

Since the Multitype Branching Processes does not include neutron population normalization, the forthcoming simulation will average fission source distribution $X_l(n)$ (defined in Eq 11) rather than the count of fission source $Z_l(n)$.

$$X_l(n) \equiv \frac{Z_l(n)}{\sum_{i=1}^{m} Z_i(n)} \tag{11}$$

The ACC of X_l between generation n and $n+k$ is defined as

$$\rho_{n,k} = \frac{Cov[X_l(n), X_l(n+k)]}{\sqrt{Var[X_l(n)]Var[X_l(n+k)]}} \tag{12}$$

Taking derivatives of moment generating fuctions in Eq 3 and Eq 9 gives expectation of products of $Z_l(n)$ such as $\mathbb{E}[Z_l(n)]$, $\mathbb{E}[Z_l(n)Z_j(n)]$ and $\mathbb{E}[Z_l(n)Z_l(n+k)]$. However, to evaluate the variance and covariance terms in Eq 12, expectations in the form of $\mathbb{E}[X_l(n)]$ and $\mathbb{E}[X_l(n)X_l(n+k)]$ are required, which must be transformed to expectations of products of $Z_l(n)$.

To perform the transformation, the definition of $X_l(n)$ (Eq 11) is viewed as a function of $\boldsymbol{Z}(n)$ and expanded around $\mathbb{E}[\boldsymbol{Z}(n)]$ $(\equiv \boldsymbol{\mu}(n))$:

$$\begin{aligned} X_l(n) &\equiv g_l(\boldsymbol{Z}(n)) = g_l(\boldsymbol{\mu}(n)) \\ &+ \sum_{i=1}^{m} \left.\frac{\partial g_l(\boldsymbol{Z}(n))}{\partial Z_i(n)}\right|_{\boldsymbol{Z}(n)=\boldsymbol{\mu}(n)} (Z_i(n)-\mu_i(n)) \\ &+ \sum_{i,j=1}^{m} \left.\frac{\partial^2 g_l(\boldsymbol{Z}(n))}{\partial Z_i(n)\partial Z_j(n)}\right|_{\boldsymbol{Z}(n)=\boldsymbol{\mu}(n)} (Z_i(n)-\mu_i(n))(Z_j(n)-\mu_j(n)) \\ &+ \cdots \end{aligned} \tag{13}$$

where the derivatives of $g_l(\boldsymbol{Z}(n))$ can be calculated from Eq 11 as

$$\left.\frac{\partial g_l(\boldsymbol{Z}(n))}{\partial Z_i(n)}\right|_{\boldsymbol{Z}(n)=\boldsymbol{\mu}(n)} = \frac{\delta_{i,l}}{\mu(n)} - \frac{\mu_l(n)}{\mu(n)^2} \tag{14}$$

$$\left.\frac{\partial^2 g_l(\boldsymbol{Z}(n))}{\partial Z_i(n)\partial Z_j(n)}\right|_{\boldsymbol{Z}(n)=\boldsymbol{\mu}(n)} = -\frac{\delta_{i,l}}{\mu(n)^2} - \frac{\delta_{j,l}}{\mu(n)^2} + 2\frac{\mu_l(n)}{\mu(n)^3} \tag{15}$$

where

$$\mu(n) \equiv \sum_{i=1}^{m} \mu_i(n) \tag{16}$$

With the expansion of $X_l(n)$ in Eq 13, the variances required to evaluate $\rho_{n,k}(X_l)$ (Eq 12) can be approximated with the expectation of products of $Z_l(n)$ in the form of $\mathbb{E}[Z_i(n)Z_j(n)]$,$\mathbb{E}[Z_i(n)Z_j(n+k)]$, $\mathbb{E}[Z_i(n)Z_j(n)Z_l(n)]$ and $\mathbb{E}[Z_i(n)Z_j(n)Z_l(n+k)]$.

It can be shown that in the expansion of the (co)variances in Eq 12, each term are on the order of $\frac{\mathbb{E}(Z_l(n)-\mu_l(n))^\alpha}{\mu(n)^\alpha}$, $\alpha \geq 2$. The expansion is valid when the system has a large number $(\mu(n))$ of expected neutrons. For example, the 3^{rd} order expansion of $Cov[X_l(n), X_l(n+k)]$ is given in Eq 17:

$$\begin{aligned} &Cov[X_l(n), X_l(n+k)] = \\ &\sum_{i,j} \left(\frac{\delta_{i,l}}{\mu(n)} - \frac{\mu_l(n)}{\mu(n)^2}\right)\left(\frac{\delta_{i,l}}{\mu(n+k)} - \frac{\mu_l(n+k)}{\mu(n+k)^2}\right) \\ &\Big(\mathbb{E}[Z_i(n)Z_j(n+k)] - \mu_i(n)\mu_j(n+k)\Big) \\ &+ \frac{1}{2}\sum_{h,i,j}\left(\frac{\delta_{h,l}}{\mu(n)} - \frac{\mu_l(n)}{\mu(n)^2}\right)\left(-\frac{\delta_{i,l}}{\mu(n+k)^2} - \frac{\delta_{j,l}}{\mu(n+k)^2} + 2\frac{\mu_l(n+k)}{\mu(n+k)^3}\right) \\ &\Big(\mathbb{E}[Z_i(n+k)Z_j(n+k)Z_l(n)] \\ &- \mu_i(n+k)\mathbb{E}[Z_j(n+k)Z_l(n)] - \mu_l(n)\mathbb{E}[Z_i(n+k)Z_j(n+k)] \\ &+ 2\mu_i(n+k)\mu_j(n+k)\mu_l(n)\Big) \\ &+ \frac{1}{2}\sum_{h,i,j}\left(\frac{\delta_{h,l}}{\mu(n+k)} - \frac{\mu_l(n+k)}{\mu(n+k)^2}\right)\left(-\frac{\delta_{i,l}}{\mu(n)^2} - \frac{\delta_{j,l}}{\mu(n)^2} + 2\frac{\mu_l(n)}{\mu(n)^3}\right) \\ &\Big(\mathbb{E}[Z_i(n)Z_j(n)Z_l(n+k)] \\ &- \mu_i(n)\mathbb{E}[Z_j(n)Z_l(n+k)] - \mu_l(n+k)\mathbb{E}[Z_i(n)Z_j(n)] \\ &+ 2\mu_i(n)\mu_j(n)\mu_l(n+k)\Big) \end{aligned} \tag{17}$$

Procedure to Calculate $\rho_{n,k}$

Knowing the spatial moments, serial moments, evolution equations and expansions of $X_l(n)$, generation-to-generation correlation coefficients, $\rho_{n,k}(X_l)$, can be calculated following the steps below:

1. Calculate the spatial moment responses M_i^l, $V_{i,j}^l$ and $W_{i,j,k}^l$
2. Evolve the spatial moments $\mu_i(n)$, $C_{i,j}(n)$ and $T_{i,j,k}(n)$
3. Combine the spatial moments of different generations to evaluate the serial-spatial moments
4. Substitute the moments into expansion of $Var[X_l(n)]$ and $Cov[X_l(n), X_l(n+k)]$ to evaluate $\rho_{n,k}(X_l)$

When evaluating the *ACC* of tally regions that are coarser than the discretized phase space, a condensation step should be inserted between step 3 and 4 which corresponds simply to the sum of the fine mesh contributions in the coarser mesh.

RESULTS AND ANALYSIS

Demonstration Problem

The simple benchmark was chosen as a 400 cm slab with vacuum boundaries and cross sections selected to mimic the migration area of a PWR as done in Ref [4]. Since the theoretical development assumes a free neutron population (i.e. no population control between generations), $\nu = 2.46425$ was selected to keep the system near critical. Future work will evaluate the impact of relaxing this assumption.

Spatial Moment Responses M_i^l, $V_{i,j}^l$, $W_{i,j,k}^l$

The spatial moment responses are calculated from the transfer matrix P, where the matrix element $P_{i,j}$ is the probability that a neutron born at phase space cell i is absorbed at phase space cell j. In this case, the phase space is discretized into 400 cells (fine enough to assume a flat source in each cell) and the matrix P is tallied from a uniformly distributed source using 200 million neutrons. Knowing the matrix P, the spatial moment responses can be calculated as

$$M_i^l = P_{l,i}\mathbb{E}\xi \tag{18}$$
$$V_{i,j}^l = P_{l,i}\delta_{i,j}\mathbb{E}\xi^2 - P_{l,i}P_{l,j}(\mathbb{E}\xi)^2 \tag{19}$$

where ξ is the random variable corresponding to the number of new neutrons created after absorption takes place, with ξ taking the following distribution:

$$\begin{aligned}
\mathbb{P}(\xi = 0) &= \frac{\Sigma_c}{\Sigma_c + \Sigma_f} \\
\mathbb{P}(\xi = 1) &= 0 \\
\mathbb{P}(\xi = 2) &= (3 - \nu)\frac{\Sigma_f}{\Sigma_c + \Sigma_f} \\
\mathbb{P}(\xi = 2) &= (\nu - 2)\frac{\Sigma_f}{\Sigma_c + \Sigma_f}
\end{aligned} \tag{20}$$

In the slab problem, the (co)variances expansion shown in Eq 17 is truncated to second order and provides sufficient accuracy. Therefore only the first and second spatial moment reponses (M_i^l, $V_{i,j}^l$) are needed.

Auto-Correlation Coefficients

With the spatial moment responses evaluated, *ACC* for any tally region l can be estimated following the steps in the last section. Verification is performed by performing 200 independent eigenvalue simulations and manually computing the (co)variances.

The results are given in Fig 1 and Fig 2 at two different tally locations, where the solid lines correspond to the *ACC* predicted by the theory of multitype branching processes and the dotted lines correspond to the *ACC* estimated from the 200 independent simulations.

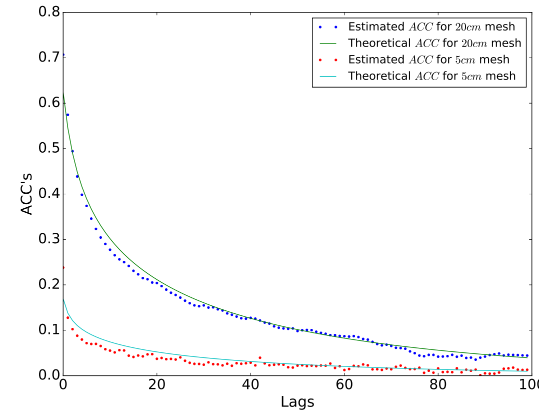

Fig. 1. *ACC* for different mesh sizes at slab boundary

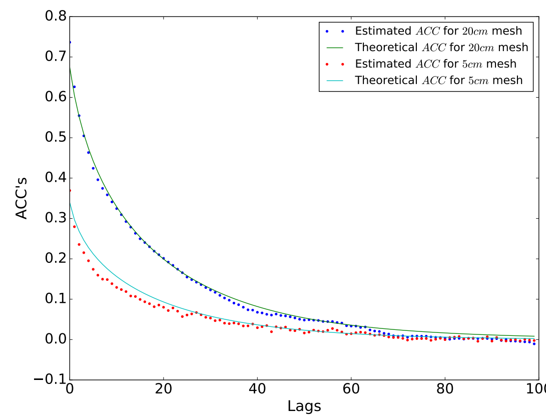

Fig. 2. *ACC* for different mesh sizes at slab center

Variance Underestimation Ratio

With the predicted *ACC*'s, the variance underestimation ratio for each tally region can be calculated [4]. The corrected variances for the boundary tally region and center tally region are plotted in Fig 3 and Fig 4. The dotted lines correspond to the variance of $\bar{X}_l$ calculated over the 200 simulations, while the green lines indicate the ideal convergence rate if neutrons were truly independent. The red lines $Var[\bar{X}_l]$ correspond to the variance predicted using the theory of multitype branching processes.

Bias of Sample Variance Estimator

Fig 3 and Fig 4 show that the theory can predict the underestimation ratio ($\equiv r$) of $Var[\bar{X}_l]$ (if approximated by $Var[X_l]/N$). However, the sample variance ($Var[X_l]$) itself is biased due to the generation-to-generation correlation [4] but can be corrected using the predicted r.

$$Var[X_l] = \frac{N-1}{N-r(N)} Var'[X_l] \tag{21}$$

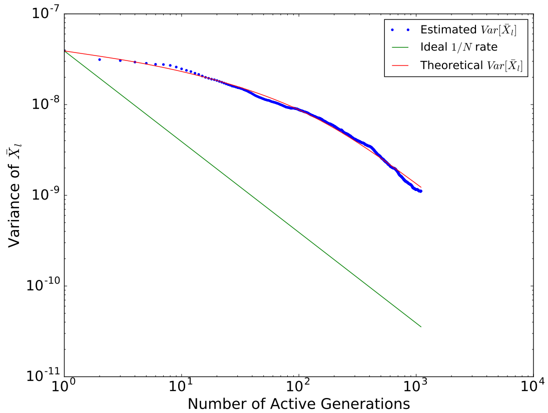

Fig. 3. $Var[\bar{X}_l]$ for $20cm$ mesh at slab boundary

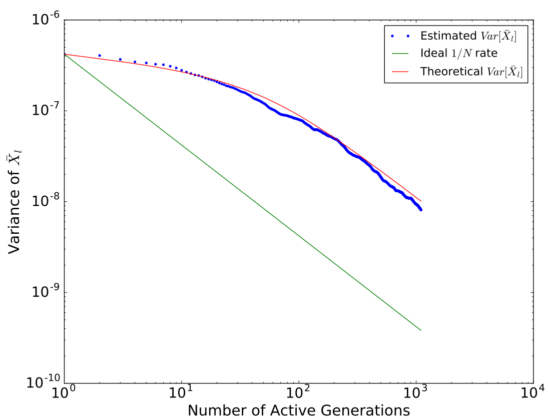

Fig. 4. $Var[\bar{X}_l]$ for $20cm$ mesh at slab center

where $Var'[X_l]$ is the sample variance of tallies of region l from N active generations. The dotted line in Fig 5 plots the ratio of sample variance ($Var'[X_l]$) estimated from various sample sizes (number of active generations) and that estimated from the largest sample size. It is consistent with the bias factor (Eq 21) predicted from ACC's.

CONCLUSIONS

Applying the theory of MBP into the discretized phase space of neutron configurations can predict the ACC's and can therefore correct the bias of sample var iance $Var[X_l]$ and the underestimation ratio of $Var[\bar{X}_l]$. Future work will include verifying the MBP method in continuous energy simulations, developing the theory for coarse DPS cells and calculating variance underestimation ratio for the uncertainty of k_{eff}. Additional work will focus on the integration of this methodology into typical Monte Carlo eigenvalue solvers using population control.

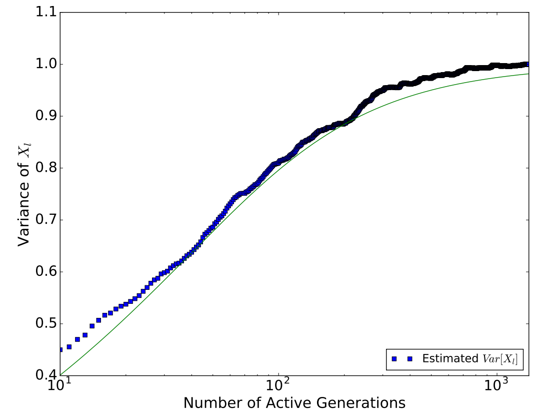

Fig. 5. Bias factor of $Var[X_l]$ for $20cm$ mesh at slab center

ACKNOWLEDGMENTS

This research was supported in part by the Consortium for Advanced Simulation of Light Water Reactors (CASL), an Energy Innovation Hub for Modeling and Simulation of Nuclear Reactors under U.S. Department of Energy Contract No. DE-AC05-00OR22725.

REFERENCES

1. R. BRISSENDEN and A. GARLICK, "Biases in the estimation of Keff and its error by Monte Carlo methods," *Annals of Nuclear Energy*, **13**, *2*, 63–83 (Jan. 1986).
2. E. DUMONTEIL, F. MALVAGI, A. ZOIA, A. MAZZOLO, D. ARTUSIO, C. DIEUDONNÉ, and C. DE MULATIER, "Particle clustering in Monte Carlo criticality simulations," *Annals of Nuclear Energy*, **63**, 612–618 (Jan. 2014).
3. B. R. HERMAN, *Monte Carlo and Thermal Hydraulic Coupling using Low-Order Nonlinear Diffusion Acceleration* , Ph.D. thesis, Massachusetts Institute of Technology (2014).
4. J. MIAO, B. FORGET, and K. SMITH, "Analysis of correlations and their impact on convergence rates in Monte Carlo eigenvalue simulations," *Annals of Nuclear Energy*, **92**, 81–95 (2016).
5. A. YAMAMOTO, K. SAKATA, and T. ENDO, "Prediction on Underestimation of Variance for Fission Rate Distribution in Monte-Carlo Calculation," *transaction of american nuclear society*, **110**, *1*, 515–518 (2014).
6. T. M. SUTTON, "APPLICATION OF A DISCRETIZED PHASE SPACE APPROACH TO THE ANALYSIS OF MONTE CARLO UNCERTAINTIES," in "ANS MC2015 - Joint International Conference Mathematics and Computation (M&C), Supercomputing in Nuclear Applications (SNA) and the Monte Carlo (MC) Method," Nashville, TN (2015), Mc, pp. 1–17.
7. C. J. MODE, *Multitype branching processes: Theory and applications*, vol. 34, American Elsevier Pub. Co. (1971).
8. H. J. SHIM, "Bias of Sample Variance and Real Variance Estimation in Monte Carlo Eigenvalue Calculations," (July 2015), presentation by Shim Hyung Jin at the Workshop on Advanced Monte Carlo Method, Kyoto University Research Reactor Institute, July 21-22, 2015.